chemosensors

MDPI

Article

Acrylamide–Fat Correlation in Californian-Style Black Olives Using Near-Infrared Spectroscopy

Antonio Fernández [1], Ismael Montero-Fernández [2], Olga Monago-Maraña [3], Elísabet Martín-Tornero [4] and Daniel Martín-Vertedor [5,*]

1 Technological Institute of Food and Agriculture (CICYTEX-INTAEX), Junta of Extremadura, Avda. Adolfo Suárez s/n, 06007 Badajoz, Spain; antonioff@unex.es
2 Environmental Engineering Agronomic and Forestry Department, University of Extremadura, Ctra. de Cáceres s/n, 06007 Badajoz, Spain; ismonterof@unex.es
3 Department of Analytical Sciences, Faculty of Sciences, National Distance Education University (UNED), Avda. Esparta s/n, Crta. de Las Rozas-Madrid, Las Rozas, 28232 Madrid, Spain; olgamonago@ccia.uned.es
4 Department of Analytical Chemistry, University of Extremadura, 06006 Badajoz, Spain; elisabetmt@unex.es
5 Department of Nature Conservation and Protected Areas, Government of Extremadura, 06800 Mérida, Spain
* Correspondence: daniel.martin@juntaex.es

Abstract: Californian-style is one of the most important black table olive elaborations. During its processing, table olives produce acrylamide, a potential carcinogen compound generated during sterilization. In the present study, total fat and acrylamide content in Californian-style table olives were determined and a regression between them was performed (acrylamide concentration range: below limit of detection—2500 ng g^{-1} and 8–22% for total fat). Nowadays, there are fast and efficient new techniques, such as Near-Infrared Spectroscopy (NIRS) to measure fat content parameters. In that sense, NIRS was used to perform a fat content quantification model in olives in order to indirectly determine acrylamide content. Calibration models for fat quantification were obtained in defatted olive pastes from a unique variety and for olive pastes from different varieties. In the first case, best results were obtained since only one variety was used (R^2 = 0.9694; RMSECV = 1.31%; and REP = 8.4%). However, in the second case, results were still acceptable R^2 = 0.678, RMSECV = 2.3%, REP = 17.7% and RMSEV = 2.17%. Regression coefficients showed the most influence variables corresponded with fat. The determination coefficient for the fat and acrylamide correlation was high (r = 0.877), being an efficient approach to find out the contribution of fat degradation to acrylamide synthesis in table olives.

Keywords: acrylamide; NIRS; table olive; fat; sterilization

Citation: Fernández, A.; Montero-Fernández, I.; Monago-Maraña, O.; Martín-Tornero, E.; Martín-Vertedor, D. Acrylamide–Fat Correlation in Californian-Style Black Olives Using Near-Infrared Spectroscopy. *Chemosensors* **2023**, *11*, 491. https://doi.org/10.3390/chemosensors11090491

Academic Editor: Jianjun Lai

Received: 6 July 2023
Revised: 21 August 2023
Accepted: 1 September 2023
Published: 6 September 2023

1. Introduction

The fruit of the olive tree (*Olea europaea* L.), when properly mature and harvested, is referred to as a "table olive". According to other researchers [1], "Manzanilla", "Gordal", "Hojiblanca", "Carrasqueña" and "Cacereña" are the most popular varieties. Even while olives are still used primarily for the manufacture of olive oil, dressings and seasonings are becoming increasingly important. The chemical composition of the olive is influenced by factors prior to the harvest, such as the type of crop, edaphic factors, environmental conditions, and the age of the tree, among others [2]. Among the main primary metabolites in table olives are fatty acids, whose main constituents are myristic, arachidic, eicosenoic, and behenic acid [3].

Depending on the processing method used, table olives may contain a lot of salt and acrylamide, a harmful chemical that should be avoided. This compound has been classified as a probable human carcinogen agent by the International Agency for Research on Cancer (IARC) [4,5]. According to the European Food Safety Authority (EFSA) [6], acrylamide increases the risk of developing cancer diseases by the consumers. Although this

dangerous chemical is usually produced in food products composed from basic materials that are heavy in carbohydrates and low in proteins, acrylamide synthesis has recently been associated with fatty meals such table olives [7]. Acrylamide appears to have been produced as a result of the high temperature required to sterilize black olives [8]. In particular, the Californian-style table olives are classified as a potential source of acrylamide [6]. This information was updated by the authorities of the member states of the European Union (EU) in the European Commission Recommendation (EU) 2019/1888, amended on 7 November 2019 [9], where olives in brine solutions were included to the list of foods in which acrylamide levels have to be taken into account.

The presence of substances that function as precursors, such as sugars and asparagine, can encourage the formation of acrylamide [10]. The generation of acrylamide during the Californian-style processing of oxidized olives was first identified by previous studies [11]; acrylamide was only discovered (243–1349 μg kg^{-1}) following sterilization. According to a different study, olive peptides may have contributed to the sterilizing process' generation of acrylamide [12]. The optimization of industrial strategies [13], the use of various ingredients and additives [14], such as phenolic compounds [15], or alternative treatments to sterilization, such as High Hydrostatic Pressure (HHP) [16] have all been studied in order to decrease or eliminate the content of acrylamide in ripe olives.

Therefore, determining the presence of acrylamide in this type of olive is a crucial factor for humans. The use of fast alternative techniques, such as Near-Infrared Spectroscopy (NIRS) is a powerful tool for qualitative and quantitative analysis to be considered. For its interpretation, multivariate analysis must be used, which leads to improved analytical applications [17]. This technique operates in the spectral regions of 800–2500 nm, and it has been considered one of the most attractive techniques of analysis for various reasons. One of them is that NIRS is a non-destructive tool that allows rapid analysis simultaneously from a wide variety of samples, such as those derived from the pharmaceutical, polymer, petrochemical, food and agricultural industries [18]; it is being used for quality control, process monitoring and estimation of useful life [19]. In the olive oil industry, it has also been used to check the adulteration of the oil as well as to differentiate between regions of different olives [20].

NIRS technique offers advantages in terms of portability and low-cost, being widely used in food quality control, as well as being a fast and non-destructive technique with minimal sample preparation [21].

One of the limitations of this technique is that the compression of the NIR spectra is not yet sufficient, since it is possible to estimate the regions of the wavenumber where modes can appear, but it is complex to explain the reasons why they occur, spectral changes or intensity alterations [22,23]. Biomolecules are a class of challenging molecules for NIR spectroscopy due to their structural complexity, as their spectra are complicated and particularly difficult for direct interpretation, as it is difficult to determine the well-defined wavenumber in ranges in which the presence of peptides, fatty acids or nucleic acids is detected [24].

With this background, the objective of the present work is to use vanguard, fast and non-expensive techniques such as NIRS to find out if there is a correlation between table olives fat content and acrylamide content, in search of a fast estimation on the toxic compound levels. The application of NIRS to Californian-style table olives to perform an early indirect determination of acrylamide concentration thanks to its total fat content has not been performed before and, for table olives, there is not much scientific literature about NIRS application and none about using this spectroscopy to determine acrylamide.

2. Materials and Methods

2.1. Olive Samples

Olives (*Olea europaea* L.) of different table olive varieties at the green ripening stage were sampled in the southwest of the Mediterranean area during the 2021–2022 crop year, in the Protected Designation of Origin Alentejo region (Portugal) and from the Scientific

and Technological Research Center of Extremadura (CICYTEX, Badajoz, Spain). After harvesting, olives were transported to the laboratories in ventilated storage trays. Harvested olives were kept in 20 L tanks for 4 months with a 3% v/v acetic acid solution. The diagram of the experiment is shown in Figure 1.

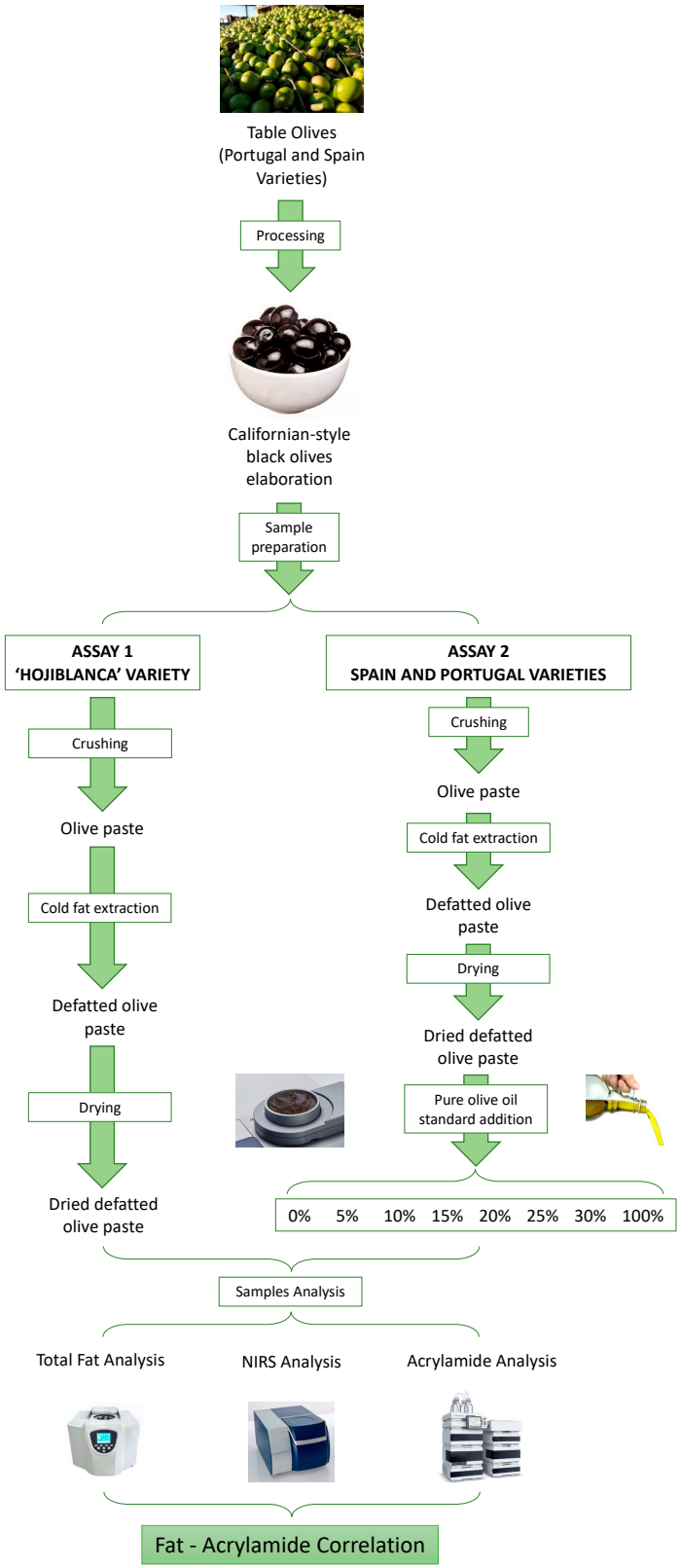

Figure 1. Diagram of the experimental design.

2.2. Manufacture Processes of Californian-Style Table Olives

Olives were processed to Californian-style black ripe olive followed the procedure explained in previous studies [25]. The stored olives were washed and subjected to a lye treatment and air oxidation treatment. Once NaOH had penetrated the olive pit, olives were neutralized (pH = 7) and a ferrous gluconate solution (1.5 g/L) was added. Using a fresh brine solution containing sodium chloride (40 g/L), ferrous gluconate (0.15 g/L), and 2 $g \cdot L^{-1}$ $CaCl_2$, washed olives were put into cans (150 g). In an autoclave set at 121 °C for 30 min (F_0 = 15 min), samples were sterilized. The olive cans were stored at dried room temperature (20 °C) until the moment of analysis.

2.3. Experimental Design

Two sets of samples were used in this study:

(i) The first was formed by Californian-style black olives from 'Hojiblanca' variety, which were first pitted and crushed with a T-18 Basis Ultra-Turrax® Homogenizer device (IKA, Staufen, Germany). After that, the fat was extracted using cold extraction protocol described in the present bibliography [26]. Then, total fat content was recorded. To continue, defatted olive samples were dried in an air circulation oven for 48 h until they had a constant weight. To perform the standard addition analysis, different concentrations of the Folch extracted fat were added to ten grams of defatted olive pastes previously weighted and prepared. Fat concentration range was the following: 0% (without any oil added), 5%, 10%, 15%, 20%, 25%, 30% and 100% (pure olive oil). Samples were prepared by quadruplicate, obtaining a total of 32 samples. The spectra were subsequently recorded by Near-Infrared Spectroscopy (NIRS).

(ii) The second set of samples was made up of olive pastes from different varieties. Olives were first pitted, crushed and total fat content was determined as in the first set. After that, ten grams of olives paste was introduced into plates to record the NIR spectra. This set consisted of a total of 96 samples.

Acrylamide content was determined for all analyzed samples.

2.4. Reference Protocols and Analysis

2.4.1. Total Fat

The Folch method was used for fat extraction with slight modifications [26]. Ten grams of olive paste were weighed in a falcon tube (Tube 1). After that, 20 mL of chloroform/methanol (2:1) was added, followed by shaking of the sample, and allowed to settle to ensure extraction. To continue, a centrifugation for 3 min at 3000 rpm was preformed and the supernatant was collected in another falcon tube (Tube 2). A total of 10 mL of chloroform was added to the sediment (Tube 1), which was mixed again to facilitate extraction. Then, it was centrifuged during 3 min at 3000 rpm and the supernatant was collected in the falcon Tube 2, where the chloroform/methanol from step 2 had been collected. Next, 10 mL of ultrapure water were added to the falcon tubes with the two supernatants (Tube 2), vortexed for 30 s, and ending with a 3 min centrifugation at 3000 rpm. The centrifugation steps were performed with a Thermo Scientific Sorvall Legend XT/XF centrifuge, with a F13-14x50c carbon fiber rotor (Thermo Fischer Scientific, Waltham, MA, USA).

The superior phase was removed with a Pasteur pipette, and the inferior phase was filtered through a paper filter with sodium sulfate anhydrous previously humidified with chloroform in an Erlenmeyer flask. Finally, the anhydrous sulfate can be washed with a small amount of chloroform to wash away any fat that may have been retained. The chloroform was evaporated from the flask using a rotary evaporator and nitrogen stream. After the evaporation, the fat content was weighed and redissolved in 2 mL of hexane. To finish, the hexane was collected with the dissolved fat in amber glass vials.

2.4.2. Near-Infrared Spectroscopy Analysis

Infrared spectra were registered with a Near-Infrared Spectrometer (Agilent Cary Series UV-VIS-NIR Spectrophotometer, Santa Clara, CA, USA). The VIS-NIRS measurements

were obtained in reflectance mode. The NIR spectra were transformed from reflectance (R) units into absorbance-like units (log (1/R)). An internal ceramic standard was used as reference. The spectrometer is equipped with a Xenon flash lamp (250 Hz) with photometric System Double beam power. The spectrum of each sample was obtained within a wavelength interval of 400–2400 nm. The spectral resolution was 0.2 nm, and the number of scans that the radiation passes through a point was 80. Table olives paste samples were measured in circular sample cups of approximately 79 cm^2 (FOSS Analytical A/S, Hillerød, Denmark). A Teflon sample was used as the reference blank. The readings were carried out in triplicate whose average reading of the spectra was used for subsequent analyses.

2.4.3. Acrylamide Analysis

The procedure outlined to extract the acrylamide from table olives was proposed by Bermudo et al. [27] and slightly modified by Pérez-Nevado et al. [8]. Two grams of homogenized olive paste were weighed, agitated for 60 min with 10 mL of Milli-Q water. The mixture was centrifuged at 1677× g/4 °C for 30 min using a Thermo Scientific Sorvall Legend XT/XF centrifuge with an F13-1450cy carbon fiber rotor (Thermo Fischer Scientific, USA). The aqueous supernatant was then filtered using a 0.45 µm nylon syringe filter (Filter-Lab, Barcelona, Spain). Disposable Telos PCX (200 mg, 3 mL) extraction columns were utilized for the solid-phase extraction. A total of 4 mL of methanol were used to condition the column before using 4 mL of Milli-Q water. The Telos PRP cartridge (60 mg, 3 mL), which had undergone the same pre-conditioning as the first cartridge, received the sample (3 mL), which was then eluted with 3 mL of Milli-Q water. High-performance liquid chromatography-triple quadrupole mass spectrometry was used to analyze the extracted (1 mL) (HPLC-MS-QQQ, Agilent Technologies, Santa Clara, CA, USA). The sample was then given 20 µL of 250 $mg \cdot g^{-1}$ acrylamide, and it was analyzed twice more after that. Milli-Q water used presented a resistivity of 18.2 $M \cdot \Omega \cdot cm$.

Agilent Technologies' Agilent 1290 Infinity II liquid chromatograph, connected to an Agilent 6460 triple quadrupole mass spectrometer, and outfitted with an Agilent Jet Stream electrospray ion source working in positive ion mode, was used to analyze samples (Agilent Technologies, Santa Clara, CA, USA). The reverse phase HPLC Zorbax XDB-C18 column (3.5 m × 150 mm × 2.1 mm) was used for elution with a 3 µL injection volume at 30 °C. The system was run in an isocratic mode at a flow rate of 0.25 mL min^{-1} for 95% of the solvent A (0.1% formic acid in Milli-Q water) and 5% of the solvent B (0.1% formic acid in methanol). The following settings were made to the ion source: 340 °C for the gas, 12 $L \cdot h^{-1}$ for the flow of the gas, 40 psi for the nebulizer, 400 °C for the sheath gas, 12 $L \cdot h^{-1}$ for the flow of the sheath gas, +2.5 kV for the capillary voltage, 300 V for the nozzle, and 300 for the delta EMV.

2.5. Multivariate Data Analysis

Calibration models for fat quantification were obtained using Partial Least-Squares (PLS) [28]. The total set of samples were randomly divided into two sets to perform the classification/quantification models. The first data set composed by the 70% of the samples (training set) was used to perform the calibration and the cross validation of the models. The other dataset (test set) was composed by the remaining samples (30% of the total samples) and it was used to test the robustness and accuracy of the developed models. The performance of the models was evaluated using the following statistic parameters: determination coefficient (R^2), root mean square error of cross-validation (RMSECV), relative error of prediction (REP) and root mean square error of validation (RMSEV).

In the case of addition standard analysis, spectra were used as raw spectra. However, mean center was needed for obtaining the models with different varieties.

Data analysis was carried out using The Unscrambler, version 6.11 (CAMO Software AS, Oslo, Norway).

2.6. Statistical Analysis

In order to predict the acrylamide level based on the total fat content of Californian-style black olives, a linear regression analysis was used. Furthermore, the statistical Spearman's correlation was calculated between both parameters. All statistical analyses were performed with IBM SPSS (Version 27.0.1.0, IBM Corp, Armonk, NY, USA).

3. Results

3.1. NIR Spectra Information

Figure 2A,B shows NIR spectra for scanning between 400 and 2500 nm of the analyzed samples for the addition standard analysis and a pure olive oil, respectively. The depressions and peaks of the spectra are observed where the characteristics of greater and lesser absorption intensity of the samples are shown. In the case of olive pastes samples, the main absorption bands are observed around 670 nm, 1209 nm, 1439 nm, 1721 nm, 1760 nm and 1935 nm. In the case of pure olive oil, the main bands appear at 670 nm, 1209 nm, 1410 nm, 1721 nm, 1760 nm, 2145 nm and 2166 nm. As observed, some of them are in consonance for both samples and pure olive oil. Moreover, by visual inspection, a clear trend is observed in some regions according to the fat content.

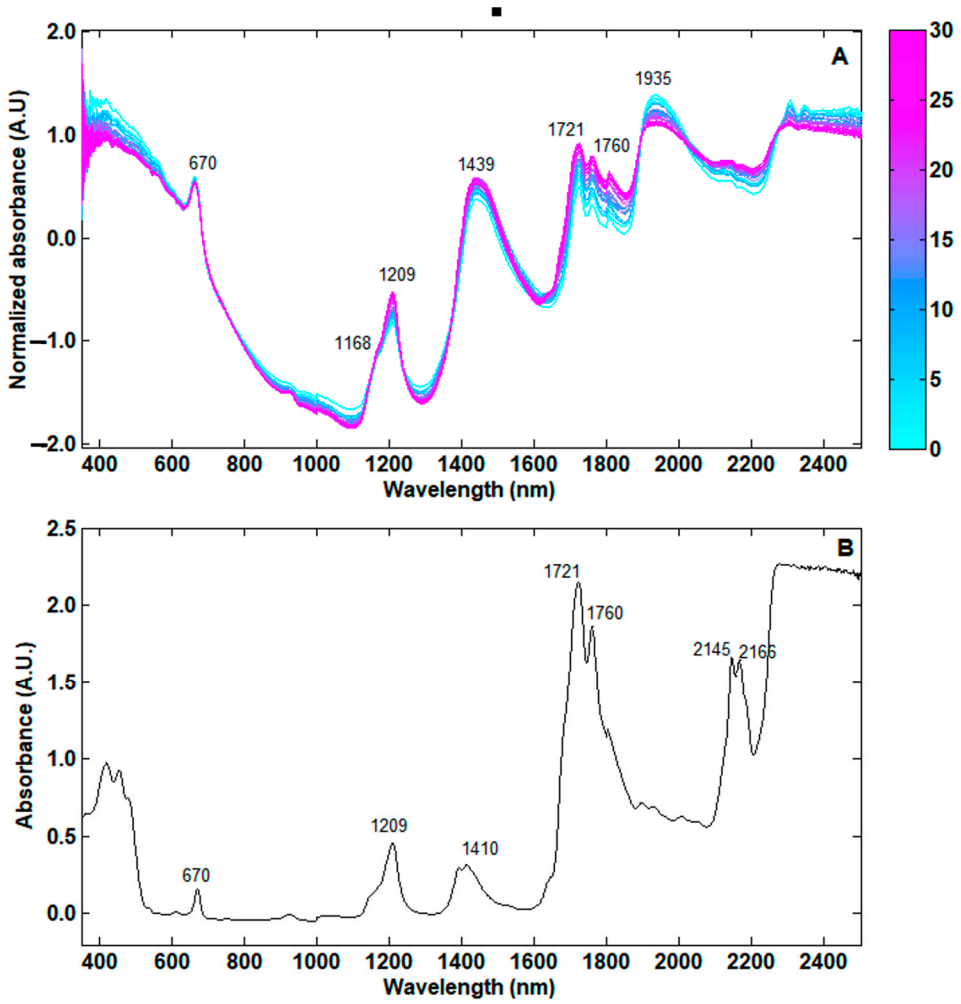

Figure 2. Pre-processed spectra for addition standard analysis (color bar represents the fat percentage) (**A**), and raw spectra for pure olive oil (**B**).

3.2. Total Fat Quantification

First, the NIR spectra were recorded for olives pastes from Californian-style black olives of the 'Hojiblanca' variety, which were doped with different concentration of fat.

PLS model was built with the data obtained. The differences among samples are due to different percentages of fat added to each sample. In this case, four components were selected as optimal, explaining the 98.2% of the total variance. Cross-validation (leaving out four samples each time) was used to evaluate the accuracy of the model and good results were obtained (R^2 = 0.9694; RMSECV = 1.31%; and REP = 8.4%). Also, regression coefficients were evaluated and are shown in Figure 3.

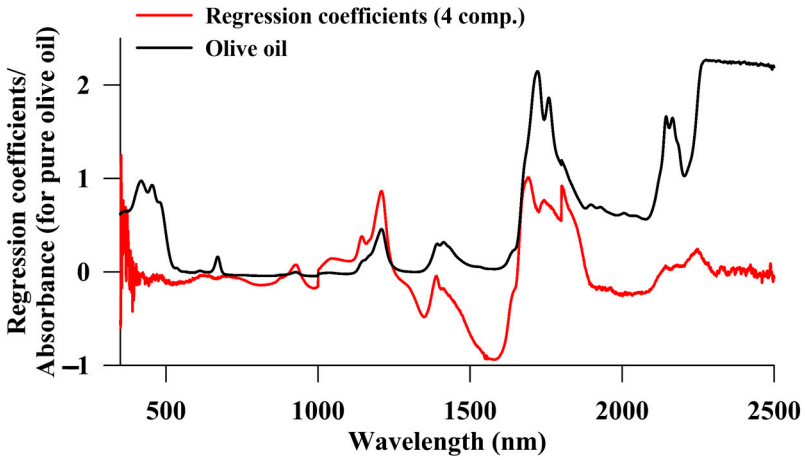

Figure 3. Regression coefficients for the model obtained for fat using one variety of olives paste with added fat (red line) and NIR spectra of pure olive oil (black line).

On the other hand, the PLS model was also built with the data of the NIR spectra of the olive pastes obtained from different varieties. Firstly, all NIR spectra data were pre-processed using Mean Center Normalization with the wavelengths ranging from 350 to 1300 nm and from 1600 to 2500 nm. Six components were required to obtain the model, explaining 75.8% of the total variance. The model offered values of R^2 = 0.678, RMSECV = 2.3% and REP = 17.7% for the cross validation and a value of RMSEV = 2.17% for the validation. These results can be considered acceptable, considering the huge variability among the different varieties. In this case, regression coefficients were also obtained and are shown in Figure 4.

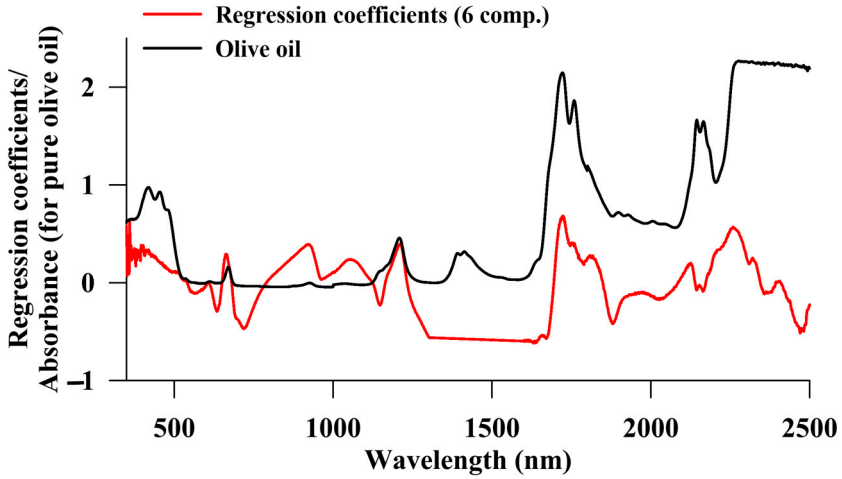

Figure 4. Regression coefficients for the model obtained for fat using different olives paste varieties (red line) and NIR spectra of pure olive oil (black line).

3.3. Relationship between Acrylamide and Fat

Regarding the previous results section, it could be pointed out that NIRS and fat content could be efficiently related, although this technique, by itself, is not enough to per-

form a direct acrylamide determination. Due to that, the correlation of fat and acrylamide content for an indirect determination was evaluated.

After the fat extraction of table olives by the method previously described in Section 2.4.1, acrylamide content in Californian-style black table olives and their fat content has been represented in the following figure (Figure 5). Looking through the regression, a direct tendency between fat content and acrylamide can be seen: the more lipidic content Californian style table olives have, the more acrylamide is generated. The regression shows an adequate linearity with a r of 0.877, a correct value to estimate a preliminary acrylamide content through fat content determination. The determination coefficient is not ideal, as there is an important acrylamide variance from some varieties to others and we are solely evaluating fat contributions to acrylamide concentration. Particularly, in the samples measured, the variety with the highest fat content presented 21.64 g of total fat and 2340 $ng \cdot g^{-1}$ of acrylamide concentration. With respect to the lower values, the variety with the lowest fat content presented 9.62 g and an acrylamide concentration of 93 $ng \cdot g^{-1}$. There have been no other studies that correlate fat content and acrylamide in Californian-style black table olives, this one being the first to approach the influence of table olives lipidic fraction to acrylamide generation. In addition, to prove the correlation was not due to random factors, a statistical Spearman's correlation analysis was performed, and this correlation (r = 0.877) was significant (p-value < 0.001) for a significance level (a) of 0.01.

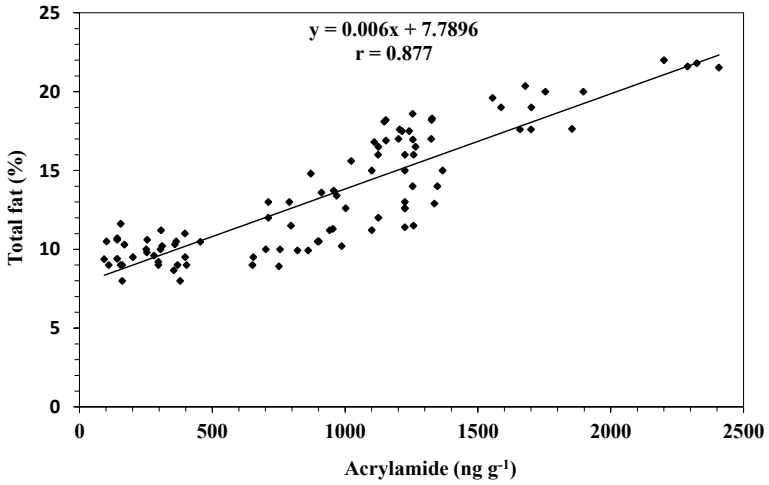

Figure 5. Spearman's linear correlation between total fat content (%) and acrylamide concentration.

4. Discussion

Regarding the spectral information from Californian-style black olives (Figure 2A) and pure olive oil (Figure 2B), it can be said that the characteristic bands between 1100 and 1500 nm are linked to the absorption of fats and oil [29]. In the wavelength range studied, the regions of 1100–1250, 1350–1500, 1700–1900, and 2100–2200 nm are the main absorption peaks responsible for discriminating saturated and unsaturated fatty acid or the oxidation of certain lipids. Additionally, the wavelength at 1209 nm is connected to $-CH_3$ and $-CH_2-$ groups of aliphatic hydrocarbon, at 1721–1760 nm are due to the first overtone of C-H from $-CH_2-$ groups and at 1392 and 1414 nm are linked to $-CH_2-$ and $-CH_3$ groups in straight alkane. For that reason, in the pure olive oil, the wavelength ranged from 2145 to 2166 nm, in which pure olive oil absorbtion can be assigned to blend bands of C-H from -HC = CH- (cis) groups of unsaturated fatty acids and C=O stretching vibration of combined spectrum band.

Furthermore, the wavelength at 670 nm is associated with chlorophyll and its derivatives [30]. Furthermore, when additional standard analysis was performed, samples with a higher percentage of fat present higher intensity bands than samples with low percentage of fat. As a result, the bands corresponding with water (at 1439 nm and 1935 nm) present an intensity inverse to the percentage of fat.

The NIRS technique has been used for years in the olive oil industry to calculate fatty yields [29]. However, until now, this equipment has not been used on California-style black olives. In this work, we have found out that this technique was able to correlate the NIR spectra with the fat content in Californian-style black olives. In this sense, researchers have indicated good correlations in fat content and other oil parameters by this technique in these samples, considering this technique a very useful tool for non-destructive analysis [31]. However, it is difficult to compare the results obtained in this study with others in the literature, because there are not many studies about olive paste; most of them are on olive oil or intact olives. For example, Salguero-Chaparro et al. [32] determined quality parameters in intact olives obtaining R^2 of 0.79 and RMSECV of 2.66%. These results are in accordance with the results from the present study. On the other hand, other researchers have obtained good results for predicting the percentages of monounsaturated, saturated and polyunsaturated fatty acids for extra virgin olive oil [33]. It can be highlighted that the excellent results ($R^2 > 0.90$) with olive oil obtained in this study might be due to the homogeneity of the samples. In another recent study, NIRS has also been used for adulteration detection of olive oil with soybean oil based on the fat composition of samples, but without quantification [30].

In this study, good results for the models were also probed when the regression coefficients were evaluated. In the case of the same variety and added fat (Figure 3), the variables that affect the most to the model were the following wavelengths: 1209 nm, 1410 nm and 1721 nm amongst others, which correspond with the main variables from pure olive oil added. In the second set of samples, which includes several varieties, when regression coefficients were evaluated (Figure 4), some variables corresponding with fat (as in the previous case) were also observed, which means that the model is based on chemical information from fat.

To continue, a good correlation was observed between the acrylamide content and the total fat. These results can be considered acceptable, considering the huge variability among different varieties and the fact that acrylamide generation probably might not occur only by fat transformation. To be more specific, there are two routes of acrylamide synthesis that have been proposed in food, which are the carbohydrates route and the fats one [34,35]. With respect to the first route, the main catalysts for the development of acrylamide are high carbohydrates foodstuffs. The precise mechanism of how acrylamide forms in food has not yet been fully understood. On one hand, most of the theories involve the breakdown of free asparagine during a Maillard reaction in heat processes like frying, baking or roasting when reducing sugars are present [36]. In this sense, it is important to highlight the low presence of table olives carbohydrates and its very low levels of asparagine and other amino acids that could be responsible of triggering this route [37]. However, additional chemical pathways may be taken within the reaction chain, leading to the formation of undesired chemicals such acrylamide, furans and (hydroxymethyl) furfural [38]. In the scientific literature, the contribution of this route to the acrylamide generation in the different food matrixes, including table olives, is well-known. In previous research, it has been thought that the main synthesis route for acrylamide in table olives might be the lipidic route, due to this fact and preliminary results [13,25].

As was observed previously in other research [23], the amounts of acrylamide in black olives oxidized to the Californian-style were much higher than those obtained in green olive processing styles. In this preliminary investigation, acrylamide values exceed 1700 $ng \cdot g^{-1}$, depending on the conditions of the sterilization process. It is important to highlight that these acrylamide values are intimately linked to the variety used, as these are more vulnerable to the sterilization process and, therefore, to generating a greater amount of the contaminant. As previously mentioned in the results section, these acrylamide concentrations correlate with a high fat concentration in table olives. Therefore, it can be affirmed that the bigger the fat content in the olive variety, the more potential acrylamide it will possess in the case of being subjected to a sterilization process. Moreover, in recent research of the group, the maturity stage of the table olive was studied with respect to

acrylamide concentration, finding higher levels of the contaminant in table olives with deeper stages of maturity. These results are in consonance with the current study, due to a higher fat content as the maturity of table olive is increases [13,39].

On the other hand, other mechanisms, like the decarboxylation of asparagine with the assistance of a specific enzyme and a cofactor in an aqueous medium, and thermolytic pathways via the Strecker aldehyde, acrolein, and acrylic acid were also proposed by Yaylayan and Stadler [40] and Granvogl et al. [41], respectively. This only leads occasionally, and to a lesser extent than the asparagine reducing sugar pathways, to the synthesis of acrylamide. In that sense, according to other researchers, one of the strongest precursor candidates is acrolein, which can be generated through lipid transformations, among others [7,34]. With that being said, table olives are considered a high fat food, which leads us to think about the importance of the contributions of this route to the acrylamide generation in Californian-style black table olives. According to previous research, this table olive elaboration present low levels of sugars [42]. For all the above, we propose that the present correlation could show before us the contribution of fat route to acrylamide levels in table olives, losing linearity according to sugar route contribution to the total quantity of acrylamide in the samples studied. Hence, considering the correlation between fat and acrylamide, this method might be used as an indirect methodology to obtain the acrylamide content approximately.

5. Conclusions

This study illustrates the feasibility of using NIR spectroscopy for quantification of indirect acrylamide in olive pastes. Firstly, calibration models for fat determination were obtained with good results for both set of samples studied and chemical information from fat was found in the regression coefficient. After that, the correlation between acrylamide and fat was evaluated, demonstrating that both chemical parameters are correlated, due to the fact that acrylamide can be synthetized by fatty acids degradation. With this, it can be said that this methodology may be a first approximation to indirect determination of acrylamide in olive pastes using a non-destructive and easy-to-use technique. In order to have a deeper understanding of the connection between fat and acrylamide, future studies should be performed with different crop year samples. This could enhance the correlation robustness and would expand the calibration model.

Author Contributions: Conceptualization, A.F., E.M-T. and D.M.-V.; Data curation, A.F., O.M.-M., E.M.-T. and D.M.-V.; Formal analysis, A.F., E.M.-T., I.M.-F. and D.M.-V.; Funding acquisition, A.F. and D.M.-V.; Investigation, A.F., I.M.-F., O.M.-M., E.M.-T. and D.M.-V.; Methodology, A.F., I.M.-F., O.M.-M., E.M.-T. and D.M.-V.; Project administration, D.M.-V.; Resources, D.M.-V.; Supervision, D.M.-V.; Validation, A.F., E.M.-T. and D.M.-V.; Visualization, A.F. and D.M.-V.; Writing—original draft, A.F., I.M.-F., O.M.-M., E.M.-T. and D.M.-V.; Writing—review and editing, A.F., E.M.-T. and D.M.-V. All authors have read and agreed to the published version of the manuscript.

Funding: This research was funded by the local government of Extremadura (ref. GR21121—AGA008) and the European Regional Development Fund (FEDER).

Institutional Review Board Statement: Not applicable.

Informed Consent Statement: Not applicable.

Data Availability Statement: The authors confirm that the data supporting the findings of this study are available within the article and the raw data that support the findings are available from the corresponding author, upon reasonable request.

Conflicts of Interest: The authors declare no conflict of interest.

References

1. Cabrera-Bañegil, M.; Martín-Vertedor, D.; Boselli, E.; Durán-Merás, I. Control of Olive Cultivar Irrigation by Front-Face Fluorescence Excitation-Emission Matrices in Combination with PARAFAC. *J. Food Compos. Anal.* **2018**, *69*, 189–196. [CrossRef]
2. Mele, M.A.; Islam, M.Z.; Kang, H.M.; Giuffrè, A.M. Pre-and Post-Harvest Factors and Their Impact on Oil Composition and Quality of Olive Fruit. *Emir. J. Food Agric.* **2018**, *30*, 592–603. [CrossRef]
3. European Commission. COMMISSION DELEGATED REGULATION (EU) 2015/1830 of 8 July 2015 Amending Regulation No 2568/91/EEC on the Characteristics of Olive Oil and Olive-residue Oil and on the Relevant Methods of Analysis. *Off. J. Eur. Comm.* **2015**, *266*, 9–13.
4. International Agency for Research on Cancer. Monographs on the Evaluation of Carcinogenic Risks to Humans: Some Industrial Chemicals. Acrylamide. In *IARC Monographs on the Evaluation of Carcinogenic Risks to Humans*; Lyons Press: Guilford, CT, USA, 1994; pp. 389–433, ISBN 9283212606.
5. World Health Organization International Agency for Research on Cancer. *IARC Monographs on the Evaluation of Carcinogenic Risks to Humans: Some Industrial Chemicals. Acrylamide*; World Health Organization International Agency for Research on Cancer: Lyon, France, 2012; Volume 100D, ISBN 978 92 832 1319 2.
6. European Food Safety Authority (EFSA). Scientific Opinion on Acrylamide in Food. *EFSA J.* **2015**, *13*, 4104. [CrossRef]
7. Pan, M.; Liu, K.; Yang, J.; Hong, L.; Xie, X.; Wang, S. Review of Research into the Determination of Acrylamide in Foods. *Foods* **2020**, *9*, 524. [CrossRef] [PubMed]
8. Pérez-Nevado, F.; Cabrera-Bañegil, M.; Repilado, E.; Martillanes, S.; Martín-Vertedor, D. Effect of Different Baking Treatments on the Acrylamide Formation and Phenolic Compounds in Californian-Style Black Olives. *Food Control* **2018**, *94*, 22–29. [CrossRef]
9. European Commission. COMMISSION RECOMMENDATION (EU) 2019/1888 of 7 November 2019 on the Monitoring of the Presence of Acrylamide in Certain Foods. *Off. J. Eur. Union* **2019**, *62*, 31–33.
10. European Food Safety Authority (EFSA). REGLAMENTO (UE) 2017/2158 DE LA COMISIÓN—de 20 de Noviembre de 2017—Por El Que Se Establecen Medidas de Mitigación y Niveles de Referencia Para Reducir La Presencia de Acrilamida En Los Alimentos. *Off. J. Eur. Union* **2017**, *304*, 24–44.
11. Casado, F.J.; Montaño, A. Influence of Processing Conditions on Acrylamide Content in Black Ripe Olives. *J. Agric. Food Chem.* **2008**, *56*, 2021–2027. [CrossRef]
12. Casado, F.J.; Montaño, A.; Spitzner, D.; Carle, R. Investigations into Acrylamide Precursors in Sterilized Table Olives: Evidence of a Peptic Fraction Being Responsible for Acrylamide Formation. *Food Chem.* **2013**, *141*, 1158–1165. [CrossRef]
13. Martín-Vertedor, D.; Fernández, A.; Mesías, M.; Martínez, M.; Díaz, M.; Martín-Tornero, E.; Martínez, M.; Díaz, M.; Martín-Tornero, E. Industrial Strategies to Reduce Acrylamide Formation in Californian-Style Green Ripe Olives. *Foods* **2020**, *9*, 1202. [CrossRef]
14. Casado, F.J.; Sánchez, A.H.; Montaño, A. Reduction of Acrylamide Content of Ripe Olives by Selected Additives. *Food Chem.* **2010**, *119*, 161–166. [CrossRef]
15. Martín-Vertedor, D.; Fernández, A.; Hernández, A.; Arias-Calderón, R.; Delgado-Adámez, J.; Pérez-Nevado, F. Acrylamide Reduction after Phenols Addition to Californian-Style Black Olives. *Food Control* **2020**, *108*, 106888. [CrossRef]
16. Lodolini, E.M.; Cabrera-Bañegil, M.; Fernández, A.; Delgado-Adámez, J.; Ramírez, R.; Martín-Vertedor, D. Monitoring of Acrylamide and Phenolic Compounds in Table Olive after High Hydrostatic Pressure and Cooking Treatments. *Food Chem.* **2019**, *286*, 250–259. [CrossRef] [PubMed]
17. Beć, K.B.; Grabska, J.; Huck, C.W. In Silico NIR Spectroscopy—A Review. Molecular Fingerprint, Interpretation of Calibration Models, Understanding of Matrix Effects and Instrumental Difference. *Spectrochim. Acta-Part A Mol. Biomol. Spectrosc.* **2022**, *279*, 121438. [CrossRef]
18. Porep, J.U.; Kammerer, D.R.; Carle, R. On-Line Application of near Infrared (NIR) Spectroscopy in Food Production. *Trends Food Sci. Technol.* **2015**, *46*, 211–230. [CrossRef]
19. Tahir, H.E.; Xiaobo, Z.; Jianbo, X.; Mahunu, G.K.; Jiyong, S.; Xu, J.L.; Sun, D.W. Recent Progress in Rapid Analyses of Vitamins, Phenolic, and Volatile Compounds in Foods Using Vibrational Spectroscopy Combined with Chemometrics: A Review. *Food Anal. Methods* **2019**, *12*, 2361–2382. [CrossRef]
20. Vanstone, N.; Moore, A.; Martos, P.; Neethirajan, S. Detection of the Adulteration of Extra Virgin Olive Oil by Near-Infrared Spectroscopy and Chemometric Techniques. *Food Qual. Saf.* **2018**, *2*, 189–198. [CrossRef]
21. Vega-Castellote, M.; Pérez-Marín, D.; Torres, I.; Sánchez, M.T. Non-Destructive Determination of Fatty Acid Composition of in-Shell and Shelled Almonds Using Handheld NIRS Sensors. *Postharvest Biol. Technol.* **2021**, *174*, 111459. [CrossRef]
22. Ozaki, Y.; Huck, C.W.; Bec, K.B. *Near Infrared Spectroscopy and Its Applications*; Elsevier: Amsterdam, The Netherlands, 2017; pp. 11–38.
23. Czarnecki, M.A.; Morisawa, Y.; Futami, Y.; Ozaki, Y. Advances in Molecular Structure and Interaction Studies Using Near-Infrared Spectroscopy. *Chem. Rev.* **2015**, *115*, 9707–9744. [CrossRef]
24. Beganović, A.; Beć, K.B.; Grabska, J.; Stanzl, M.T.; Brunner, M.E.; Huck, C.W. Vibrational Coupling to Hydration Shell—Mechanism to Performance Enhancement of Qualitative Analysis in NIR Spectroscopy of Carbohydrates in Aqueous Environment. *Spectrochim. Acta-Part A Mol. Biomol. Spectrosc.* **2020**, *237*, 118359. [CrossRef] [PubMed]
25. Martín-Vertedor, D.; Fernández, A.; Mesías, M.; Martínez, M.; Martín-Tornero, E. Identification of Mitigation Strategies to Reduce Acrylamide Levels during the Production of Black Olives. *J. Food Compos. Anal.* **2021**, *102*, 104009. [CrossRef]

26. Kozłowska, M.; Gruczyńska, E.; Ścibisz, I.; Rudzińska, M. Fatty Acids and Sterols Composition, and Antioxidant Activity of Oils Extracted from Plant Seeds. *Food Chem.* **2016**, *213*, 450–456. [CrossRef]
27. Bermudo, E.; Moyano, E.; Puignou, L.; Galceran, M.T. Determination of Acrylamide in Foodstuffs by Liquid Chromatography Ion-Trap Tandem Mass-Spectrometry Using an Improved Clean-up Procedure. *Anal. Chim. Acta* **2006**, *559*, 207–214. [CrossRef]
28. Paul, G.; Bruce, R.K. Partial Least-Squares Regression: A Tutorial. *Anal. Chim. Acta* **1986**, *185*, 1–17.
29. Alamprese, C.; Grassi, S.; Tugnolo, A.; Casiraghi, E. Prediction of Olive Ripening Degree Combining Image Analysis and FT-NIR Spectroscopy for Virgin Olive Oil Optimisation. *Food Control* **2021**, *123*, 107755. [CrossRef]
30. Meng, X.; Yin, C.; Yuan, L.; Zhang, Y.; Ju, Y.; Xin, K.; Chen, W.; Lv, K.; Hu, L. Rapid Detection of Adulteration of Olive Oil with Soybean Oil Combined with Chemometrics by Fourier Transform Infrared, Visible-near-Infrared and Excitation-Emission Matrix Fluorescence Spectroscopy: A Comparative Study. *Food Chem.* **2023**, *405*, 134828. [CrossRef]
31. Armenta, S.; Moros, J.; Garrigues, S.; De La Guardia Cirugeda, M. Determination of Olive Oil Parameters by Near Infrared Spectrometry. In *Olives and Olive Oil in Health and Disease Prevention*; Elsevier: Amsterdam, The Netherlands, 2010; pp. 533–544, ISBN 9780123744203.
32. Salguero-Chaparro, L.; Baeten, V.; Fernández-Pierna, J.A.; Peña-Rodríguez, F. Near Infrared Spectroscopy (NIRS) for on-Line Determination of Quality Parameters in Intact Olives. *Food Chem.* **2013**, *139*, 1121–1126. [CrossRef]
33. Cayuela, J.A.; García, J.F. Sorting Olive Oil Based on Alpha-Tocopherol and Total Tocopherol Content Using near-Infra-Red Spectroscopy (NIRS) Analysis. *J. Food Eng.* **2017**, *202*, 79–88. [CrossRef]
34. Ehling, S.; Hengel, M.; Shibamoto, T. Formation of Acrylamide from Lipids. *Adv. Exp. Med. Biol.* **2005**, *561*, 223–233. [CrossRef]
35. Xu, X.; An, X. Study on Acrylamide Inhibitory Mechanism in Maillard Model Reaction: Effect of p-Coumaric Acid. *Food Res. Int.* **2016**, *84*, 9–17. [CrossRef]
36. Liu, J. Acrylamide Is Formed in the Maillard Reaction. *J. Sci. Food Agric.* **2018**, *98*, 448–449. [CrossRef]
37. Rocha, J.; Borges, N.; Pinho, O. Table Olives and Health: A Review. *J. Nutr. Sci.* **2020**, *9*, e57. [CrossRef]
38. Friedman, M. Acrylamide: Inhibition of Formation in Processed Food and Mitigation of Toxicity in Cells, Animals, and Humans. *Food Funct.* **2015**, *6*, 1752–1772. [CrossRef] [PubMed]
39. Fernández, A.; Martillanes, S.; Lodolini, E.M.; Martínez, M.; Arias-Calderón, R.; Martín-Vertedor, D. Effect of Elaboration Process, Crop Year and Irrigation on Acrylamide Levels of Potential Table Olive Varieties. *J. Sci. food Agric.* **2023**, *Online ahead of print*. [CrossRef] [PubMed]
40. Yaylayan, V.A.; Stadler, R.H. Acrylamide Formation in Food: A Mechanistic Perspective. *J. AOAC Int.* **2005**, *88*, 262–267. [CrossRef]
41. Granvogl, M.; Jezussek, M.; Koehler, P.; Schieberle, P. Quantitation of 3-Aminopropionamide in Potatoes—A Minor but Potent Precursor in Acrylamide Formation. *J. Agric. Food Chem.* **2004**, *52*, 4751–4757. [CrossRef]
42. Kerimi, A.; Nyambe-Silavwe, H.; Pyner, A.; Oladele, E.; Gauer, J.S.; Stevens, Y.; Williamson, G. Nutritional Implications of Olives and Sugar: Attenuation of Post-Prandial Glucose Spikes in Healthy Volunteers by Inhibition of Sucrose Hydrolysis and Glucose Transport by Oleuropein. *Eur. J. Nutr.* **2019**, *58*, 1315–1330. [CrossRef]